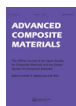


This article was downloaded by: [Chongqing University]

On: 14 February 2014, At: 06:59

Publisher: Taylor & Francis

Informa Ltd Registered in England and Wales Registered Number: 1072954 Registered office: Mortimer House, 37-41 Mortimer Street, London W1T 3JH, UK



## Advanced Composite Materials

Publication details, including instructions for authors and subscription information:

<http://www.tandfonline.com/loi/tacm20>

### Full-scale static test of small composite aircraft

Jae-Yeul Shim<sup>a</sup> & Seokmin Ahn<sup>b</sup>

<sup>a</sup> Aircraft Structures Team, Korea Aerospace Research Institute, 169-84 Gwahak-ro, Yuseong-gu, Daejeon 305-806, Republic of Korea

<sup>b</sup> Aeronautical Technology Division, Korea Aerospace Research Institute, 169-84 Gwahak-ro, Yuseong-gu, Daejeon 305-806, Republic of Korea

Published online: 29 Nov 2013.

To cite this article: Jae-Yeul Shim & Seokmin Ahn (2014) Full-scale static test of small composite aircraft, *Advanced Composite Materials*, 23:1, 85-98, DOI: [10.1080/09243046.2013.862391](https://doi.org/10.1080/09243046.2013.862391)

To link to this article: <http://dx.doi.org/10.1080/09243046.2013.862391>

PLEASE SCROLL DOWN FOR ARTICLE

Taylor & Francis makes every effort to ensure the accuracy of all the information (the "Content") contained in the publications on our platform. However, Taylor & Francis, our agents, and our licensors make no representations or warranties whatsoever as to the accuracy, completeness, or suitability for any purpose of the Content. Any opinions and views expressed in this publication are the opinions and views of the authors, and are not the views of or endorsed by Taylor & Francis. The accuracy of the Content should not be relied upon and should be independently verified with primary sources of information. Taylor and Francis shall not be liable for any losses, actions, claims, proceedings, demands, costs, expenses, damages, and other liabilities whatsoever or howsoever caused arising directly or indirectly in connection with, in relation to or arising out of the use of the Content.

This article may be used for research, teaching, and private study purposes. Any substantial or systematic reproduction, redistribution, reselling, loan, sub-licensing, systematic supply, or distribution in any form to anyone is expressly forbidden. Terms & Conditions of access and use can be found at <http://www.tandfonline.com/page/terms-and-conditions>

## NOTE

### Full-scale static test of small composite aircraft

Jae-Yeul Shim<sup>a\*</sup> and Seokmin Ahn<sup>b</sup>

<sup>a</sup>*Aircraft Structures Team, Korea Aerospace Research Institute, 169-84 Gwahak-ro, Yuseong-gu, Daejeon 305-806, Republic of Korea;* <sup>b</sup>*Aeronautical Technology Division, Korea Aerospace Research Institute, 169-84 Gwahak-ro, Yuseong-gu, Daejeon 305-806, Republic of Korea*

(Received 28 January 2013; accepted 23 August 2013)

This paper addresses the accuracy of test load application and reaction prediction of aircraft full-scale static test. Factors which have an effect on the accuracy of load application have been identified. An effective procedure for installing test article and actuators is proposed to achieve accurate loading direction compared to conventional one. A method to define quality of load control for a full-scale static test is suggested by using root mean square deviation (RMSD) of command-feedback (CMF) values. Test result of U1 test condition for the KC-100 full-scale static test has shown 8.7 N of averaged RMSD value. At the end, an approach to make general equation for reaction to load increment has been presented and reaction can be assumed to have relation of linear to load increment for symmetric load condition. The linear behavior has been shown through a test data of the KC-100 aircraft which has high stiffness of composite material structure. The test result presents that the linear behavior of the reaction has been well corresponding to the linear model.

**Keywords:** full-scale static test; KC-100; test system; test frame; test load control error; reaction load; restraint system; root mean square deviation (RMSD); command-feedback (CMF)

#### 1. Introduction

Full-scale static tests of a small composite aircraft (KC-100) were performed in KARI. Full-scale structure tests are required to show structural integrity of an aircraft for design load during developing the aircraft.

There are typical engineering works in preparing and performing aircraft full-scale static test. Those works include test load generation, design test systems, preparation of test equipment, and operating test. There are not many papers related to full-scale structure tests.[1–4] All these papers are focused on introducing design concept of test systems such as loading system, counterbalance system, restraint system, etc. No papers are found to address test static accuracy for full-scale structure static test which requires complicated test systems.

There are several factors related to the accuracy for full-scale static test. Those factors are related to test load generation and test load application to test article. Test load is decided by aircraft designer within some percent error compared to design load through VMT (Shear Force, Bending & Torsional Moment) comparison, while the test load application's accuracy related to direction and magnitude of test load depended on

---

\*Corresponding author. Email: [jyshim@kari.re.kr](mailto:jyshim@kari.re.kr)

test engineer's work and procedure quality. The test load generation is not involved in this study.

Because the accuracy of loading direction depends on the installation of test article and loading system, the process of these installations needs to be managed well to achieve high accuracy. Reference point and base lines in real testing space not in CAD space are needed to achieve accurate loading direction. On the other hand, key factor which has an effect on load magnitude is quality of load control.

An effective procedure, which makes reference and base lines in testing space through three-dimensional measuring device and applies the measuring results into CAD design for achieving accurate installation of loading system, has been proposed in this paper.

It is not simple to define test accuracy in a full-scale static structure test which generally requires dozens of control channels. A definition of accuracy required to analyze quality of test control in a full-scale static test is proposed, and the KC-100 full-scale static test data are analyzed through the definition in this paper.

Restraint system is one of test systems required for conducting an aircraft full-scale structure test and restricts rigid body movement of test article during the test. Restraint system consists of six sets to restrict 6 DOF of the test article. Each set has a load cell monitoring the reaction during testing. Because the reaction is also one of the loads applied to test article during test, it is very desirable to predict the reaction as test load increases during performing test. Since there has been no publication of study on the reaction prediction, a method to make an equation for the reaction is proposed for a full-scale static structure test. And the method is verified through the KC-100 full-scale static test data in this study.

## 2. Test article and test systems

Test article is generally whole airframe structure for an aircraft full-scale test except some structures proven by other independent tests and non-structural parts. The excluded parts carrying load in an airframe should be replaced by dummies for the full-scale test. The test article of KC-100 aircraft for static test is shown with the air-

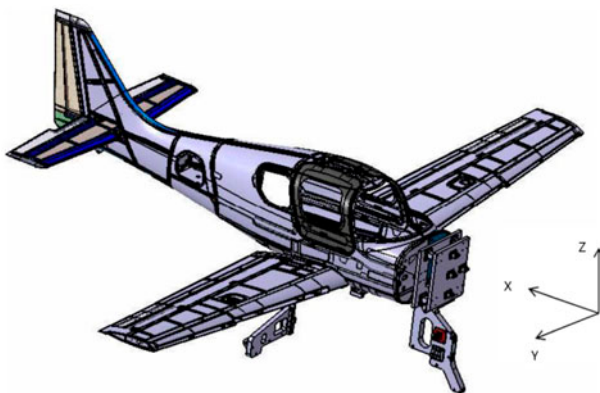


Figure 1. Test article with some dummy structures.

craft coordinate in Figure 1. The test article includes dummy landing gears, engine mount system (EMS) and engine, etc.

Important test systems designed to perform an aircraft full-scale test include restraint system and loading system. And test frame is also generally required to perform accurately an aircraft full-scale static test.

Test frame surrounds the KC-100 test article installed on a restraint system and is shown in Figure 2. The detailed restraint system for the test is shown in Figure 3 and consists of six spring-link assemblies. Each spring-link assembly has two springs. Each assembly has a load cell to monitor reaction caused while testing.

A typical loading system consisted of strap and whiffle-tree is shown in Figure 4. The loading system applies test load to test article through an actuator which is mounted to the frame. The strap is installed correctly on the test article with installing lines (line-1 and -2) shown in Figure 5. Therefore, the accuracy of loading direction largely depends on the accuracy of installation of the test article, loading system, and actuator. Since total 22 test conditions are existed for the KC-100 full-scale static test and each test condition needs its own load distribution to test article, loading system and actuator are changed at every test condition for the test. Therefore, it is emphasized to manage accurate installation of loading system and actuator in process of changing set-up for the next load condition test to achieve accurate test. As an example, a typical loading system to test article with restraint system is shown in Figure 6 for the first load condition U1. Total 23 loading actuators (which are active control channels in control) are used for this condition. There are always six reactions (which are passive monitor channels) in the restraint system for this test. The test load for the U1 is shown in Table 1 where the 'Test load (N)' and 'Total (N)' are based on the sign of the aircraft coordinate shown in Figure 1 and the load cell sign convention, respectively. Positive and negative sign corresponds to tension and compression load in load cell sign convention, respectively. Test load data were recorded by load cell sign convention. Sign of the test load data should be transformed to the corresponding value in the

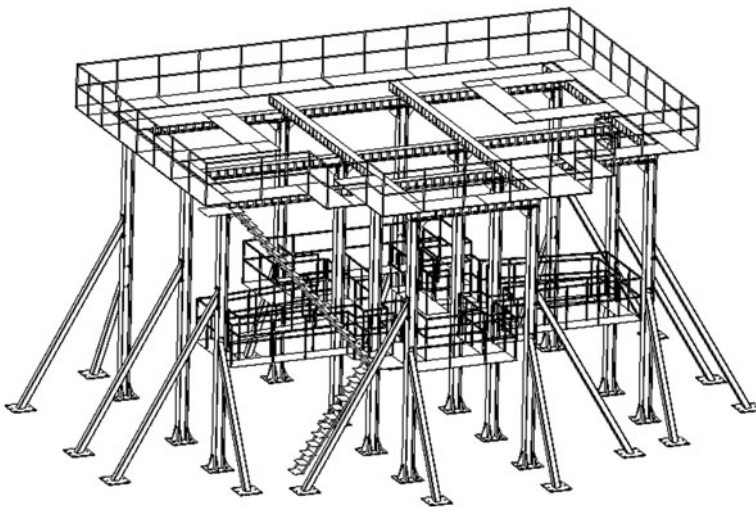


Figure 2. Test frame with ladder and working support.

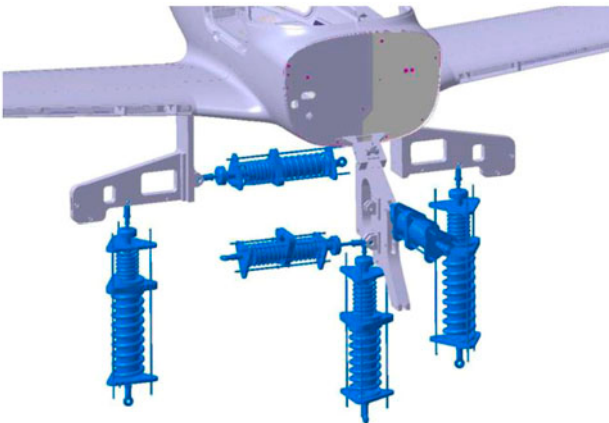


Figure 3. Test article on restraint system.

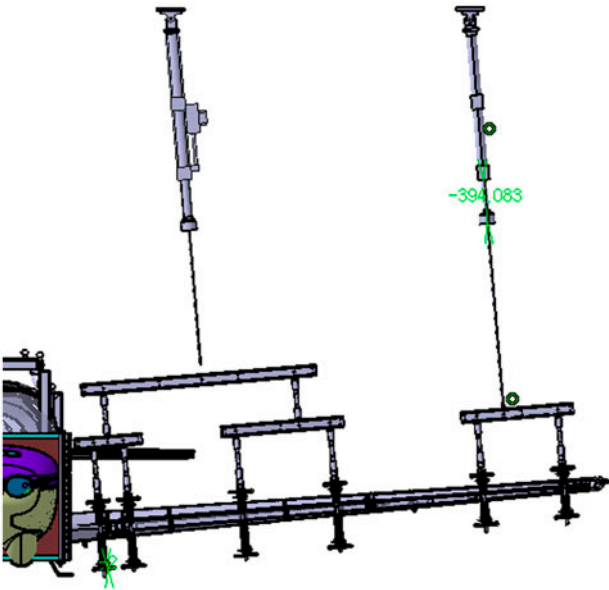


Figure 4. Typical pulling type whiffle-tree for wing boxes.

aircraft coordinates for applying the test data into equilibrium equation to calculate reactions.

The reactions are intended to be zero for the U1 condition at zero load i.e. 0% DLL (design limit load). This means that all test loads are balanced themselves at zero load for this condition. Reactions will be analyzed from the test data and equilibrium equations in the following chapter.

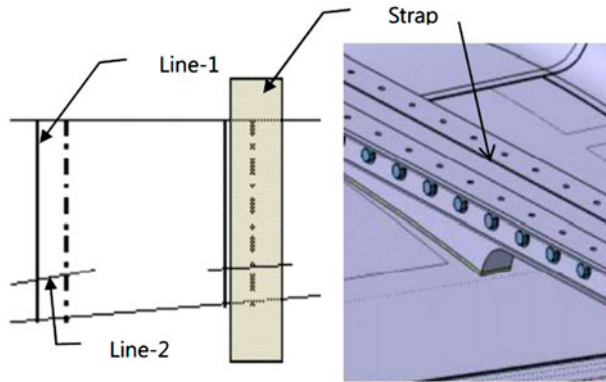


Figure 5. Strap installation lines.

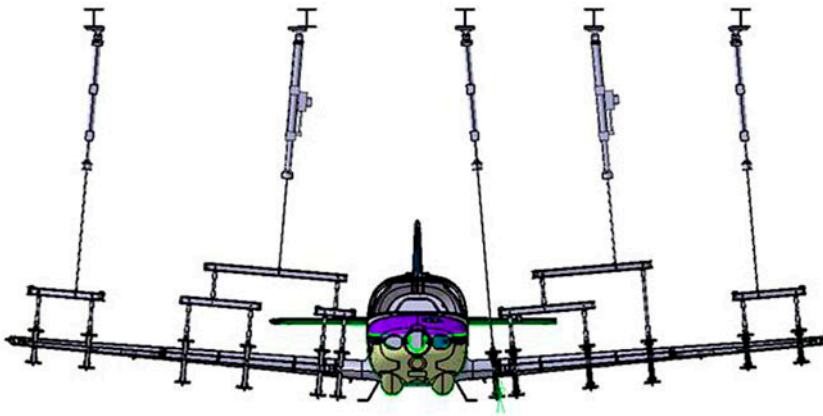


Figure 6. Loading system for wing of U1 test condition.

### 3. Accuracy of load application

Test load accuracy can be evaluated by direction and magnitude of load application to test article. Loading direction is decided from installation of test article, loading system, and actuator. Loading magnitude depends on load control accuracy and load cell calibration characteristics. The accuracy of the installation and load control is described in this chapter.

As shown in Figure 4, the accuracy of loading direction depends on installation of test article, strap, whiffle-tree, and actuator. Because straps are installed on the skin of the test article which has marked lines on the test article surface (Figure 5), those are assumed to be installed correctly as designed. And because the parts of whiffle-tree were designed by solid model tools like CATIA and manufactured by CAM machine, the geometry error of the parts can be also assumed to be negligible. And whiffle-tree is simply and correctly installed for the loading system. Therefore, the installation of test article and actuator can be identified to be important for achieving accurate loading direction.

Table 1. Test load of control channels for U1 test.

Loading system ID			T. Ch	A/T ID	Test loads (N)		Total (N)
					Limit	Ultimate	
Main wing box	Left	MWB_L_UP_F_IN	7	99	2947	4421	4421
		MWB_L_UP_F_MID	8	97	3465	5197	5197
		MWB_L_UP_F_OUT	9	101	3328	4992	4992
Flap		FLAP_L_LW	10	18	3113	4670	-4670
Aileron		AIL_L_LW	11	114	1454	2181	-2181
Main wing box	Right	MWB_R_UP_F_IN	12	22	9898	14,847	14,847
		MWB_R_UP_F_OUT	13	100	1769	2654	2654
Flap		FLAP_R_LW	14	17	3125	4688	-4688
Aileron		AIL_R_LW	15	115	1088	1632	-1632
Fuselage	Vert	F_V_FWD_EMS	16	10	-10,014	-15,022	-15,022
		F_V_FWD_FWBKHD	17	110	-3033	-4550	4550
		F_V_CNTR_PILOS	18	11	-7931	-11,897	-11,897
		F_V_PASS_FNT	19	112	-1966	-2950	-2950
		F_V_AFT_FIT	20	1002	1051	1577	1577
	Side	F_V_AFT_REARBKHD	21	95	-2733	-4099	-4099
		F_S_L_FWD	22	15	-1829	-2744	2744
		F_S_R_FWD	23	109	1142	1713	1713
		F_S_L_AFT	24	8	-3252	-4878	4878
		F_S_R_AFT	25	7	3675	5512	5512
H/T box	Left	HTB_L_LW	26	94	-2756	-4134	4134
	Right	HTB_R_LW	27	16	-2690	-4035	4035
V/T box	Left	VTB_L	28	1001	-991	-1487	1487
	Right	VTB_R	29	111	1391	2087	2087

An effective process is developed for installation of the test article and actuator for a full-scale structure test for achieving high accuracy. The process is as follows:  
It is necessary to define basis (points, lines) first in working space for installing test article and actuators.

- Define and mark a reference point (0, 0) on test floor shown in Figure 7.

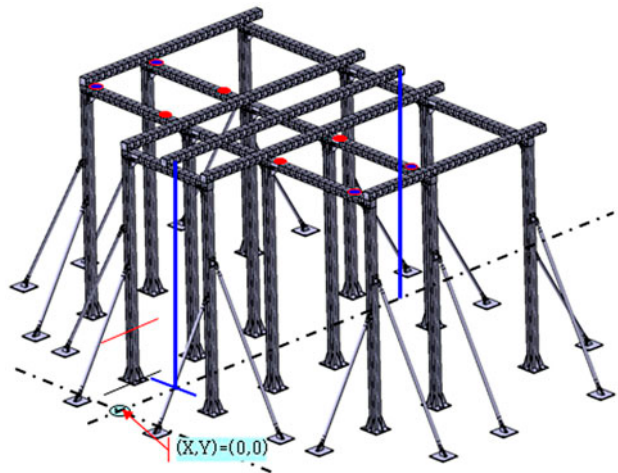


Figure 7. Base points and lines for installation of test article and actuator.



- Define and mark  $X$ - and  $Y$ -axis lines on the floor.
- Install test frame on the floor with the point and lines.
- Mark measured points on the columns, longitudinal and transverse beams by using a 3-D measuring device like laser tracker (Figure 7) .

Test article will be installed accurately on the designed space without problem by matching between station lines on skin of test article and the corresponding distance from the measured points on floor and test frame. The station lines on the skin must be prepared during assembly process of test article.

The test frame designed initially in computer was updated with the measured coordinates of points for installing actuators. Actuator installation point is defined by using the updated computer model to keep accurate loading direction. This method is more effective than conventional method in which columns and transverse and longitudinal beams are to be correctly installed as possible as it can be. This conventional method needs massive works with measuring tool to install elements within tight error band to achieve high accuracy. The process of the two methods is shown in Figure 8 where left is conventional method.

Installation error of test article and actuator was managed within  $\pm 2.5$  mm for this test.

Load control characteristics which decide loading magnitude are explained in this section.

Test data are planned to be scanned at every ‘♦’ mark in the 150% DLL test profile shown in Figure 9, and was scanned when all control channels are reached within tolerant error which is defined for every channel differently. The tolerant error is called by static null pacing error in the control system.

Test results for the U1 test condition which has 23 control channels are shown in Table 2 and Figure 10. The command-feedback (CMF) in Table 2 is magnitude of an error in engineering unit for each control channel and is ‘command-feedback.’ The

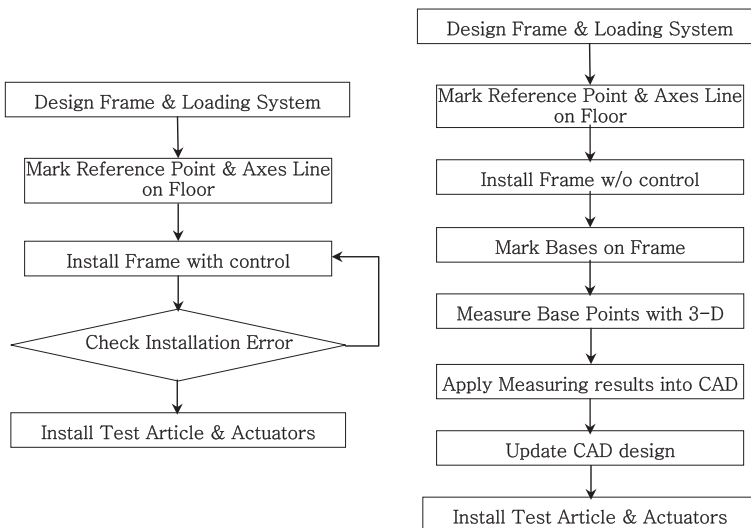


Figure 8. Two processes for Installation of test article and actuators.



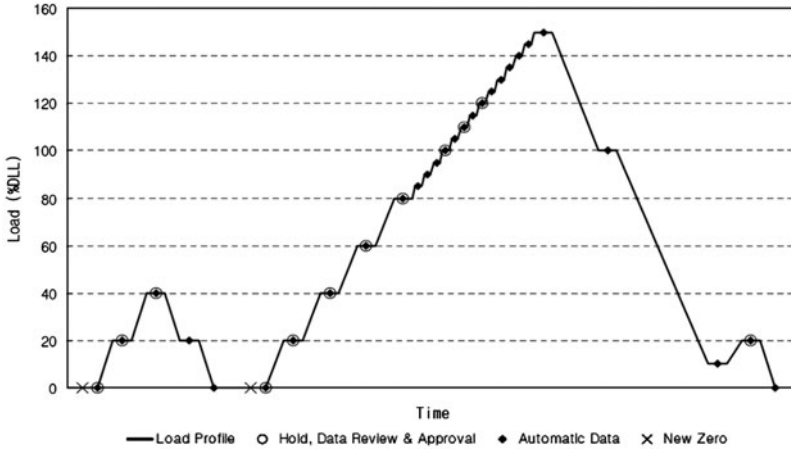


Figure 9. Standard test profile for 150% DLL test.

command is load magnitude corresponding to percent load based on the test load in the last column in Table 1. There are many factors to affect load control quality such as skill of controller operator, characteristics of loading system, actuator, and servo valve. Even though controller operator performs tuning process for all control channels during test preparation to minimize control error, the error is always existed. Therefore, tolerance of error should be defined before starting test.

Root mean square deviation (RMSD) of CMFs is applied for the first time to evaluate quality of load control in this paper. The RMSD is calculated by Equation (1) with CMF values of 23 channels for a scanned load data. The RMSD of CMFs to % DLL is shown in Figure 11, and the average value of the RMSDs for U1 test was 8.6 N which can be evaluated as very small.

$$\text{RMSD} = \sqrt{\sum_i^n \frac{(\text{CMF})_i^2}{n}} \quad (1)$$

As mentioned at the last sentence of Chapter 2, reactions could be calculated theoretically and simply through six equilibrium equations with magnitude, point, and direction of load. In the process of generating test load, reactions were calculated by the equilibrium equations with un-deformed configuration of test article. According to the calculation, reaction was zero. However, the reaction data in real test may not be zero, which is caused from not only tolerant error of load control, installation of test article and loading system, load cell calibration but also test article deformation which changes as load increases. The reactions should be monitored with tolerance limit during test to protect over load to test article. Therefore, it is very useful to provide prediction tool for the reaction of a test.

The reactions can be related to terms in Equation (2) which is based on the equilibrium equations. The first term is related to change of loading direction for active control channels. The change of loading direction is shown in Figure 12 where,  $f$ ,  $\alpha$ ,  $\xi$  and  $h_0$  are force, angle, initial distance from a reaction point to loading point, initial distance between an actuator loading point to test article, and actuator pivot point, respectively. The second term is related to change of counterbalance loading direction shown in Figure 13 where  $F$ ,  $\alpha$ ,  $\eta$ , and  $H_0$  are initial counterbalance error, angle, initial distance between a reaction point and counterbalance loading point, and initial distance

Table 2. CMF values of 23 control channels to DLL (unit, N).

T. Ch	DLL, %																						
	0	20	40	60	80	85	90	95	100	105	110	115	120	125	130	135	140	145	150	100	10	20	0
7	3	5	-10	1	7	-5	7	-4	2	2	10	3	6	-10	-6	12	-3	-5	7	3	0	-3	-10
8	-9	3	-3	13	-4	11	4	9	3	-7	4	6	7	7	13	1	4	42	41	-3	4	1	-4
9	35	13	-18	16	-17	21	14	3	-13	3	-9	16	13	-6	8	1	7	36	7	-8	-17	8	0
10	0	0	0	-3	0	-5	0	-1	-1	-2	0	-2	0	-1	0	2	-1	0	0	1	1	-1	2
11	3	-1	0	9	8	5	7	-9	-9	-10	-7	9	7	-8	6	0	-5	10	9	-3	-1	1	-1
12	-12	-12	7	2	17	16	-5	-7	3	-3	10	5	3	17	12	-5	3	16	43	9	-3	21	-30
13	0	1	-3	-8	1	-2	-3	9	13	8	-3	1	-3	-7	-1	0	-1	1	-5	2	3	3	1
14	-3	-2	6	0	6	7	-2	-7	-13	-4	8	6	7	3	3	-7	-7	-4	-1	0	0	-3	5
15	0	1	1	-4	-1	-5	-10	10	14	11	-6	-5	-5	-4	2	-5	-7	-4	-7	4	4	-4	1
16	-10	-2	2	9	0	2	2	-2	2	5	2	-2	7	-3	0	7	-5	-2	10	7	3	3	9
17	2	2	1	2	2	2	-1	-4	0	8	3	-11	12	15	1	-3	-4	14	-11	-4	-1	2	-19
18	3	-2	7	-5	-9	5	2	3	-2	2	-2	0	0	0	0	-5	-5	-17	-33	7	2	-3	-5
19	5	-1	2	-3	-2	-16	-3	-4	1	7	-10	7	-1	3	0	13	-2	-7	-11	0	-4	-2	2
20	0	0	1	2	-3	1	0	1	1	-1	-1	4	2	-1	3	-1	2	3	1	-1	0	2	-4
21	3	0	0	0	-4	0	-1	-2	-3	-3	1	-1	-1	-1	-3	-7	-10	-8	-7	1	1	-4	2
22	3	0	1	2	4	-3	3	3	-2	2	10	4	-8	-9	-4	2	4	-3	-2	-8	2	-1	-4
23	2	0	0	-1	-6	-1	-4	-5	2	2	10	5	-10	-9	-13	-2	-1	-3	5	-22	-12	-1	2
24	0	1	1	2	-3	0	1	0	-1	0	0	-1	-3	-2	1	2	3	0	3	0	0	0	0
25	-1	1	2	-3	-1	-1	0	3	0	-1	1	1	4	3	-3	1	0	2	3	-1	1	0	-1
26	11	0	0	2	2	-2	-2	-4	-3	2	1	3	4	-4	3	1	9	3	7	0	4	1	0
27	-2	0	0	-2	0	1	-1	0	0	0	-2	2	1	0	-2	2	-1	0	-3	1	1	0	-1
28	-3	0	-1	-1	-2	0	1	0	-1	0	-1	5	0	1	1	0	-3	-1	0	1	-1	-1	-2
29	-1	1	0	0	-1	0	-1	1	1	1	-1	1	-1	1	-1	0	-2	0	1	-2	0	1	0

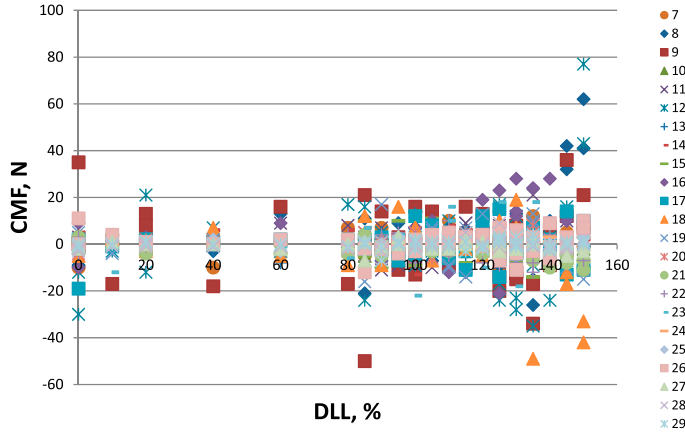


Figure 10. CMF for 231 control channels.

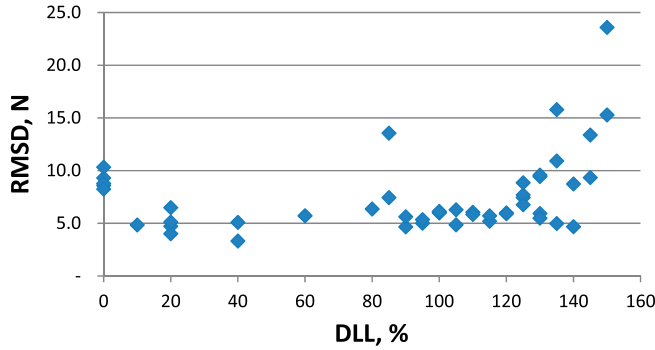


Figure 11. RMSD of 23 CMFs to load level.

between counterbalance loading point and pivot point of pulley, respectively. The Equation (2) can be expressed by Equation (3) after simple manipulation of terms. The Equation (3) can be simplified by Equation (4) for small angle  $\alpha$  with similar order between  $\xi$  (or  $\eta$ ) and  $h_0$  (or  $H_0$ ). Because counterbalance load is only applied by dead weight–pulley assembly shown in Figure 13, counterbalance load magnitude  $F$  is not changed during test. While, test load  $f$  should be expressed by Equation (5) where  $f_{\text{cmd}}$ ,  $f_{\text{cal error}}$ , and  $f_{\text{cmf}}$  are command force, calibration error in force, and CMF, respectively. Because load cell with high linearity characteristics is used for the test, the calibration error can be assumed to be linear to load increment. Therefore,  $f_{\text{cmd}}$  and  $f_{\text{cal error}}$  are changed linearly by load increment. While  $f_{\text{cmf}}$  depends on quality of load control and does not depend on load increment. Finally, the reaction can be expressed by Equation (6) after putting  $f$  in Equation (5) into Equation (4). The equation has linear to load increment ( $\Delta P$ ). The first term in Equation (6) is constant for load increment due to initial counterbalance error and the second term can be calculated from CMF values of control channels due to control error at any moment.

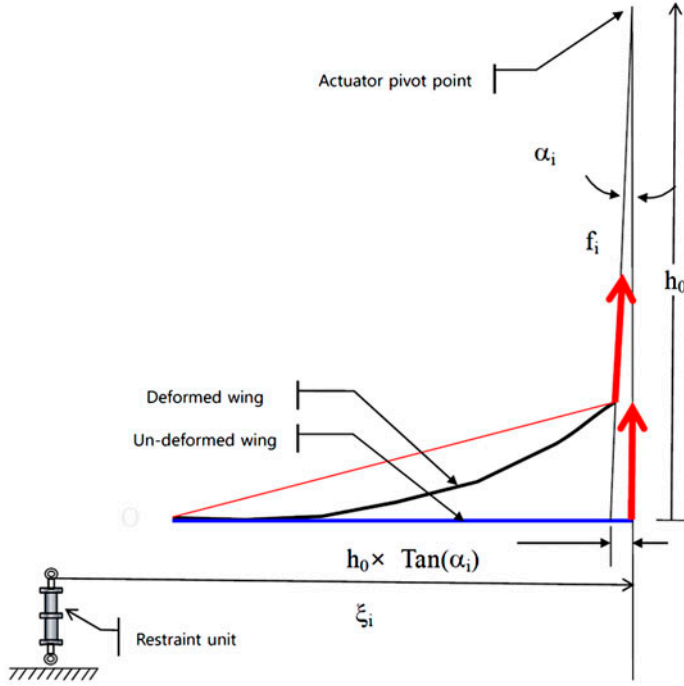


Figure 12. Change of loading direction due to wing deformation.

$$R^j \sim \left( \sum_i^n f_i \cos \alpha_i \times (\xi_i - h_0 \tan \alpha_i)_0^i + \sum_k^m F_k \cos \alpha_k \times (\eta_k - H_0 \tan \alpha_k)_0^i \right) / l, \quad j = 1 \sim 6 \quad (2)$$

$$R^j \sim \sum_i^n f_i \frac{(\xi_i \cos \alpha_i - h_0 \sin \alpha_i)}{l} + \sum_k^m F_k \frac{(\eta_k \cos \alpha_k - H_0 \sin \alpha_k)}{l} \quad (3)$$

$$R^j \sim \sum_i^n f_i \frac{\xi_i (\cos \alpha_i)}{l} + \sum_k^m F_k \frac{\eta_k (\cos \alpha_k)}{l} = \sum_i^n f_i \frac{\xi_i}{l} + \sum_k^m F_k \frac{\eta_k}{l} \quad (4)$$

$$f = f_{\text{cmd}} - f_{\text{cmf}} + f_{\text{cal error}} = C_1(\Delta P) + C_2(\Delta P) - f_{\text{cmf}} = C_3(\Delta P) - f_{\text{cmf}} \quad (5)$$

$$R^j \sim R_0^j + R_{\text{cmf}}^j + C(\Delta P)^j, j = 1 \sim 6 \quad (6)$$

Because wing stiffness of a composite aircraft is generally higher than metallic aircraft, the reaction can be presented by linear function of load increment ( $\Delta P$ ) like Equation (6) from the assumption of small deformation of wing displacement which induces to small angle ( $\alpha$ ).

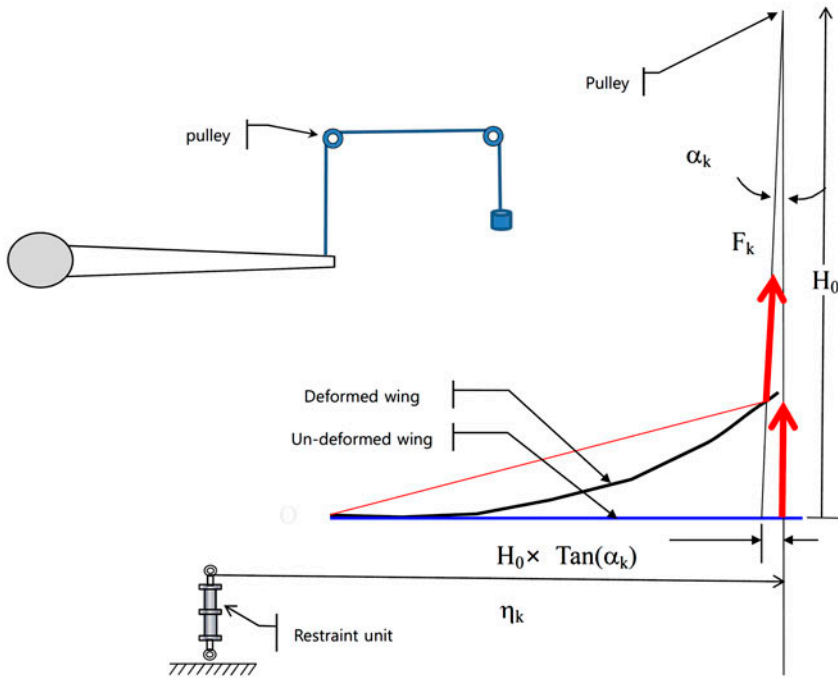


Figure 13. Change of counterbalance loading direction due to wing deformation.

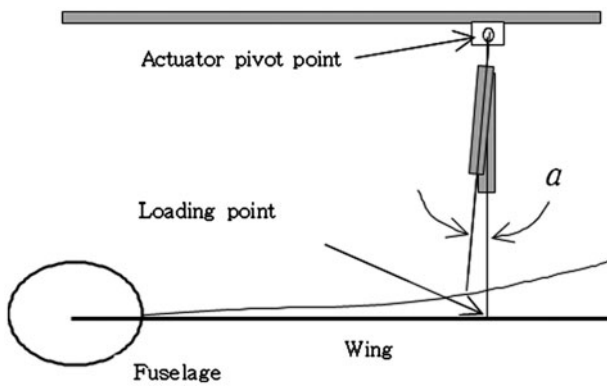


Figure 14. Angle between two loading directions.

Let us check the angle ( $\alpha$ ) from U1 test data to verify the assumption of small angle. This angle was evaluated simply from the test results of wing displacement as follows:

The displacement near wing tip (at  $y = 5410$  mm) of U1 test condition was measured by 198 mm, and initial length between actuator pivot point and loading point is about 4335 mm. The loading point is the reflected point to wing neutral line shown in Figure 14. Deformed shape of wing is assumed by linear instead of curvature for

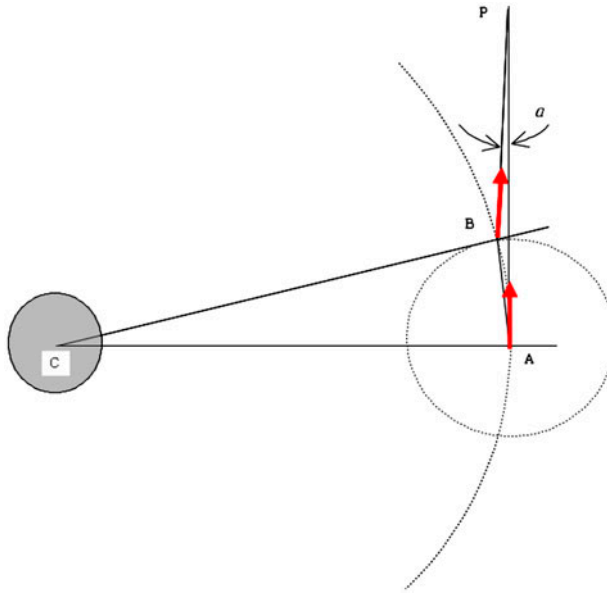


Figure 15. Angle ( $\alpha$ ) analysis from geometry and displacement.

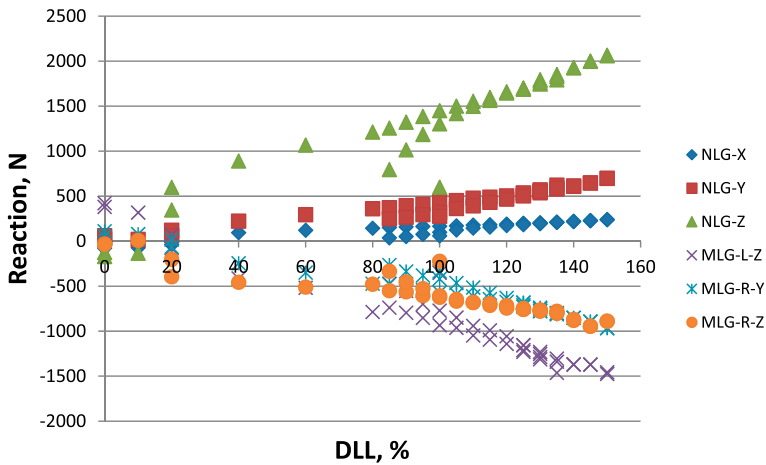


Figure 16. Measured reaction values for U1 test.

evaluating angle  $\alpha$  for simple calculation. The angle  $\alpha$  for this condition was  $0.05^\circ$  which are measured from the real scale geometry from schematic drawing shown in Figure 15. First draw a circle from center point C with radius 5410 mm which is distance to loading point A for an actuator; second draw a circle from center point A with radius 198 mm. The point B is decided at an intersection point of two circles. The two loading directions ( $P_A$ ,  $P_B$ ) from pivot point P were drawn, and then the angle  $\alpha$  was reading in CATIA. Since  $\zeta(\eta)$  and  $h_0$  ( $H_0$ ) are similar order of distances and sine ( $\alpha$ ) and cosine ( $\alpha$ ) are 0.00087 and 1.0, respectively, the reaction related to be linear

for load increment ( $\Delta P$ ) shown in Equation (6), may be reasonable for this test condition U1 with small deformation. The reactions recorded in the test condition U1 show linear behavior to load increment as shown in Figure 16. The reaction in Figure 16 shows some fluctuations above 130% DLL which is due to CMF values fluctuation shown in Figure 10. This relationship between CMF value and reaction can be explained by the second term of Equation (6).

It is generally needed to derive explicit equation of the reaction for calculating maximum reaction values before testing. However, the maximum reactions can be also easily estimated by extrapolation based on the linear relation which can be found through low level test results like 40% DLL test. Predicted maximum reaction will be checked to be within tolerant limit for the structural safety reason before starting 150% DLL test.

The derivation of explicit equation for the reaction is not included in this study and will continue for the next study.

#### 4. Conclusions

This paper addresses accuracy and reaction of full-scale static test which has some decades of loading channels. Accurate installation of test article and loading system is required to achieve higher test accuracy. A procedure for installing test article and loading system with actuator is developed and is explained to be more effective than conventional method. This is realized by updating actuator attachment points through applying measurement result of frame installation into CAD design. The installation error was within  $\pm 2.5$  mm for the KC-100 full-scale static test for the new procedure.

A way to define accuracy of test control for a full-scale static test which has some dozens of loading channels is proposed with RMSD of CMF values. The mean RMSD value of this test condition U1 is 8.6 N which can be estimated to be very accurate.

An approach to find equation for the reaction of a full-scale static test is introduced; the reaction has relation of linear to load increment for the small deformation. It is desirable to find explicit equation for the reaction to expect maximum reaction value for the test. It will continue to find the explicit equation for the reaction for future study.

#### References

- [1] Shim JY, Kim SJ, Kim SC, Hwang IH. Full-scale static test of advanced trainer aircraft. In: KSAS 2002 Fall Conference; 2002 Nov; Pyeong Chang, Korea. p. 385–389.
- [2] Shim JY, Kim SC. Full-scale static test of 4 seats canard type composite aircraft. In: US–Korea Conference (UKC) 2007; 2007 Aug; Washington (DC). AST-3.2.
- [3] Shim JY, Lee SG, Ahn SM. KC-100 full-scale static test system. *Aerosp. Eng. Technol.* 2012;11-1:7–18.
- [4] Jung JK, Lee KB, Yang MS, Shul CW. A study on the test load simulation technique for T-50 full scale durability test. *J. Korean Soc. Aeronaut. Space Sci.* 2004;32–3:82–87.